Chapter 5

Gadolinium and Terbium Metal Films and Surface Oxides

The unique electronic and magnetic properties of lanthanides result from the presence of a highly localized partially filled 4f shell. The open 4f shell is responsible for the large localized magnetic moments. While the 4f shell maintains atomic character in the metallic phase, the 5d6s band states are responsible for metallic bonding. For magnetic order, a direct exchange mechanism can be ruled out due to the negligible overlap of 4f states on neighboring lattice sites. Yet, polarization of conduction electrons by 4f moments leads to an indirect exchange mechanism, in which the delocalized valence-band electrons mediate interaction between the localized 4f moments via the so-called Ruderman-Kittel-Kasuya-Yosida (RKKY) exchange interaction, although their contribution to the total magnetic moment is small. This interaction mechanism, in competition with magneto-crystalline anisotropies and magnetoelastic energies, leads to the formation of complicated magnetic structures as, e.g., ferromagnetic, helical antiferromagnetic, and conical ferrimagnetic spin structures [45, 46] in RE metals.

The fundamental interest in rare-earth metals is further enhanced by the unique interplay between the highly localized 4f states and the itinerant valence electrons, which – in particular – can result in different electronic and magnetic properties at surfaces and interfaces as compared to the rather well-known bulk properties.

5.1 Structure and magnetic properties of Gd and Tb metal films

The starting point for the results presentation of this work will be a close inspection of the morphology, crystal structures, and the magnetic properties of thin films of Gd and Tb on a W(110) substrate.

Deposition of Gd on W(110), followed by annealing at the appropriate tem-

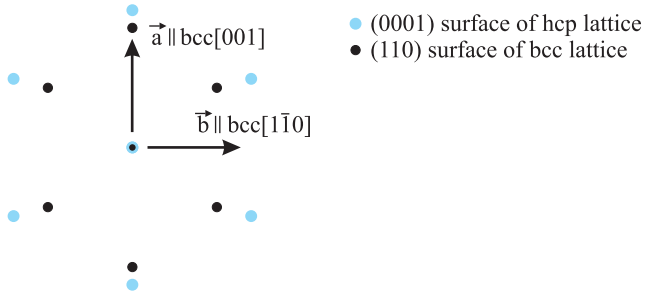

Figure 5.1: Comparison of atomic positions in the (0001) surface of the RE hcp lattice with the structure of the bcc (110) surface lattice of W(110).

perature, results in smooth films with monoatomically stepped surfaces. However, further annealing causes the Gd film to break up into 3D islands with quasi-hexagonal shapes and relatively uniform sizes that form on a first epitaxial monolayer of Gd. The optimum annealing temperature depends on the thickness of the Gd film [27, 47, 48]. The direction $\vec{a}$ (which points along the in-plane n.n. direction) is parallel to the W[001] direction, as shown in Fig. 5.1.

At the initial stage of adsorption in the submonolayer regime on W(110), Gd forms several different phases, in which interatomic spacings vary with coverage, leading to the formation of $(n \times 2)$-structures with n=10, 8, 7, 6, 5 [49]. One monolayer is found to form a complicated (7×14) lateral superstructure due to the incommensurability of the Gd and W lattices [26].

For thin films, the resulting strain of the Gd lattice relaxes by incorporating dislocations in the second and the following layers.

A recent STM study [49] has shown that the lattice parameter of the epitaxial system Gd/W(110) in the first two layers is larger than of bulk Gd. The lattice mismatch amounts to 2 % for the first and 0.3 % for the second monolayer, reaching the bulk value in the third layer. Moreover, a layer thickness dependent STS investigation of the Gd surface state splitting demonstrates that the splitting changes only below 4-ML thickness but remains constant above [50]. This behavior was interpreted in the following way: the surface stress in epitaxially grown Gd(0001)/W(110) films decreases with increasing coverage, whereby the film surface approaches the equilibrium lattice constant of an unstrained hcp(0001) surface of bulk Gd.

A study of the surface crystal structure of 400-Å-thick Gd(0001) films by LEED-I-V measurements, in combination with dynamical LEED calculations, found an inward relaxation of the surface layer by 2.4 % and an expansion of the second-layer spacing by 1 % [48]. This result is in good agreement with values determined for the (0001) surface of bulk Gd crystals [51].

Deposition and growth of Tb on W(110) is in many respects similar to that of Gd [52]. The annealing temperature for a 10-nm Tb film is noticeably higher than for Gd films (880 K vs. 650 K). This is not surprising if one remembers that cohesive energy and melting point are slightly higher for Tb than for Gd. The LEED intensity analysis of the (0001) surface of a bulk Tb crystal [51] reveals

that this surface is also relaxed, with the first interlayer spacing contracted by 3.9 % and the second one expanded by 1.4 % as compared to the bulk value.

Gadolinium is often considered as a prototype ferromagnet with localized magnetic moments (Heisenberg ferromagnet), where the half filled 4f shell ($S = 7/2,\ L = 0$) gives rise to the localized large spin-only magnetic moment of $\simeq 7\mu_B$ per lattice site. The ferromagnetic/paramagnetic phase transition of Gd occurs at the Curie temperature of $T_C = 293.4$ K. Because the half-filled 4f shell has a spherical charge distribution, magnetic anisotropy is two to three orders of magnitude smaller than for other lanthanide metals [53].

The easy axis of the hcp Gd lattice exhibits a temperature dependence. In the temperature range between 240 K and T_C, the easy axis is along the c axis; below 240 K it continuously turns away from the c axis up to a maximum angle of about 65°, that is reached at ≃170 K, and then turns back towards 30° off the c axis at very low temperatures [53]. Concerning the magnetization of thin Gd films on W(110), there is in general consensus that the demagnetization field keeps the magnetization in the film plane, even though the magnetic anisotropies favor a magnetization component out-of-plane. For film thicknesses above 350 Å , a Gd film on W(110) exhibits a canted magnetization (i.e. with a non-zero component perpendicular to the surface); but this effect has not been observed for film thicknesses below 250 Å.

Bulk Tb crystals exhibit a helical magnetic structure in the temperature range from $T_N = 232$ K to $T_C = 219.5$ K, with the magnetic moments oriented in the basal plane and the axis of the helix pointing along the c axis [53]. In the ferromagnetic phase below 219.5 K, the b-axis becomes the easy axis of magnetization. The non-spherical charge distribution of the 4f orbital wave function causes a strong magneto-crystalline anisotropy. Thus, as for the Gd films studied in this work, the easy axis of magnetization lies in the surface plane.

Although an antiferromagnetic coupling between bulk and surface has been claimed [54] and was subsequently theoretically proposed in the past [55], and also a possible canting of the surface magnetization has been suggested [56,57], it is generally believed today that the surface 4f moments of Gd(0001) are coupled ferromagnetically to the bulk moments [58,59].

In light of the controversial results concerning the alignment of surface and bulk magnetic moments, it is worthwhile to look at the magnetic properties of a pure Gd metal film. MCD in core-level photoemission provides direct information on the relative orientation of the surface and bulk 4f moments.

The MCD 4f-spectra of a 10 nm-thick Gd(0001) metal surface are presented in Fig. 5.2. Upon reversal of the film magnetization from nearly parallel to antiparallel with respect to photon spin (light propagation direction), the relative intensities of the Gd-4f ^7F multiplet components clearly change. In the experimental spectra one can recognize the rather peaked and rounded line shapes, corresponding to the multiplet intensities for $\Delta M = +1$ and $\Delta M = -1$ transitions from the fully magnetized Gd-4f shell (see inset); for a derivation of the theoretical multiplet intensities, see section 4.4. In addition, one can also see that the spectra contain a double-peaked structure. This double-peaked structure arises from the well-known surface core-level shift of the 4f lines for

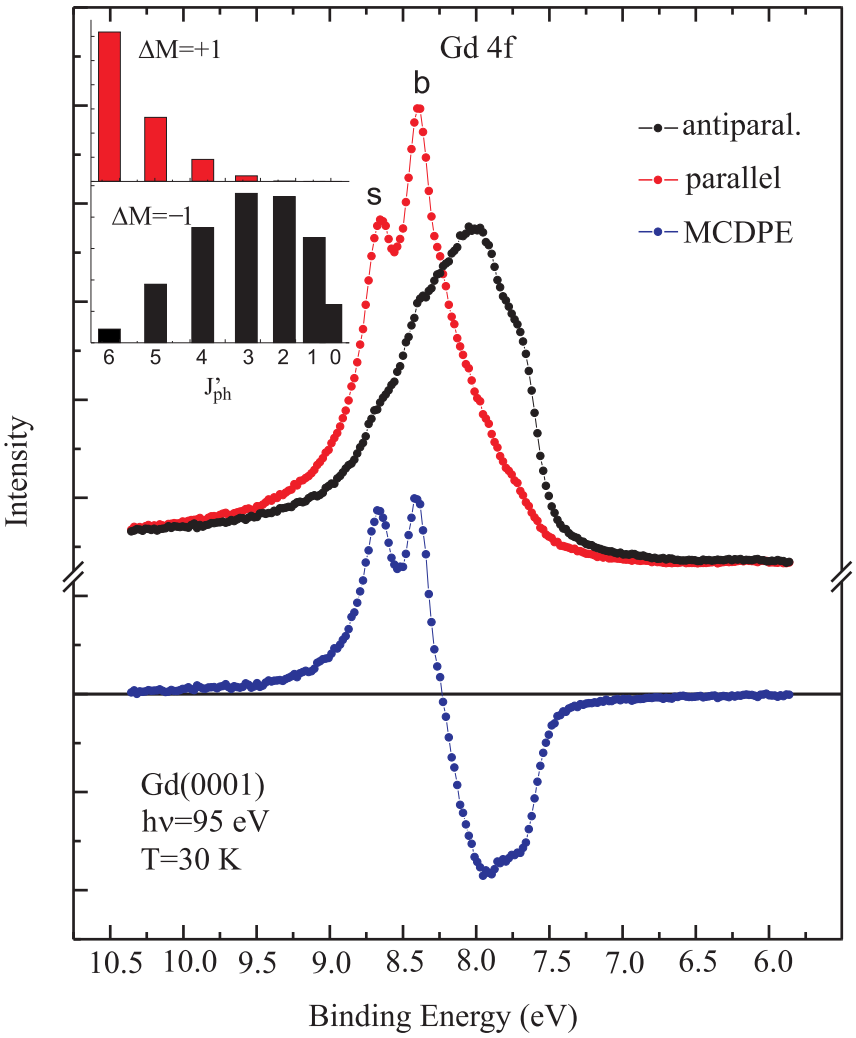

Figure 5.2: 4f PE spectra of a remanently magnetized 10-nm thick Gd(0001)/W(110) film at T = 30 K, excited with circularly polarized light for nearly parallel (red) and antiparallel orientation (black) of sample magnetization and photon spin (light incidence angle $\theta^{h\nu} = 15°$, acceptance angle of electron analyzer defined in Fig. 3.7 $\alpha = \pm 14°$). Spectral components are marked as s for surface and b for bulk. The lower panel gives the difference spectrum. The relative intensities of the ^7F multiplet components for $\Delta M = +1$ and $\Delta M = -1$ transitions are given in the inset.

atoms which have a different coordination number (number of nearest neighbors) [60, 61]. The 4f component associated with the top layer of the metal surface (line s in Fig. 5.2) is shifted by 0.28 eV to higher binding energies with respect to the bulk line (surface core-level shift [61]). This shift permits a separate study of the surface and bulk orientations of 4f moments. For these MCD in PE measurements, the samples were magnetized in the film plane along the b direction of the hcp lattice.

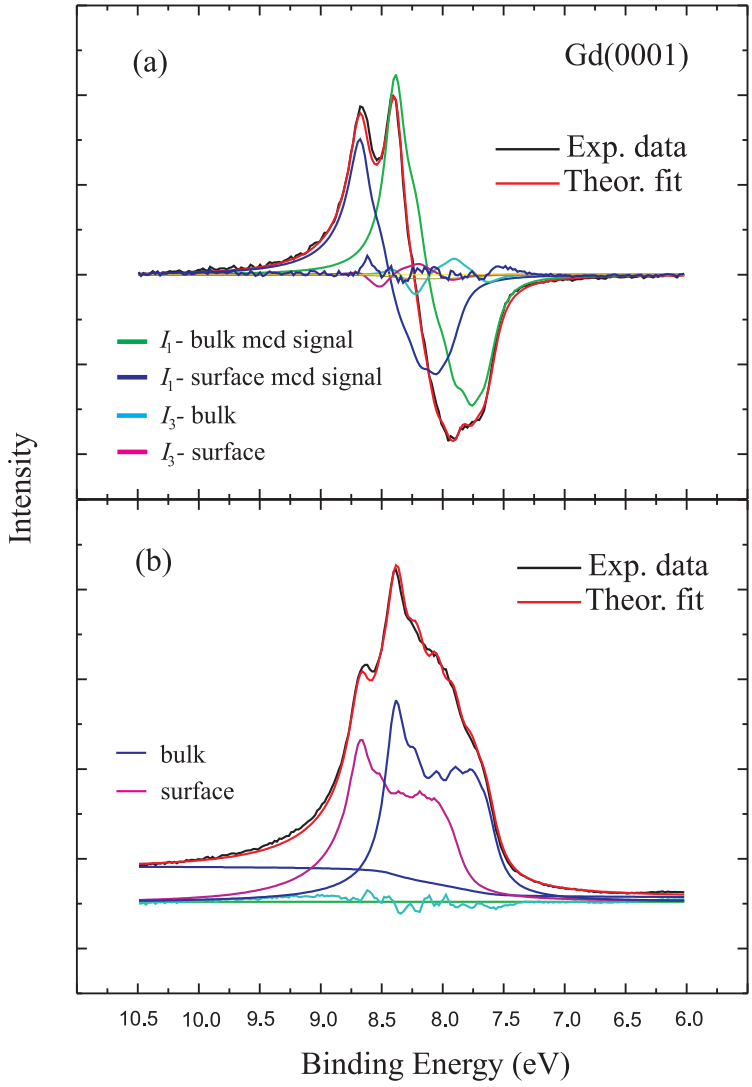

Figure 5.3: (a) Results of the simultaneous fit analysis of the spectra shown in Fig. 5.2. Experimental data are represented by solid black curves; fit - thin red curves; residuum - blue curve (noisy curve approx. the zero line). First order components, proportional to the magnetization: bulk (narrower), surface (broader). Thin curves of the small amplitudes represent the small higher-order contributions to the PE line intensity. (b) Fit analysis of the sum of the two spectra in Fig. 5.2 measured for opposite magnetizations (red and black) used to determine the ratio of intensities of the surface and the bulk component.

As described in Section 4.4 the total line strength of the Gd 4f lines does not depends on light polarization (consequence of the $L = 0$ ground state). This allows a convenient way of normalizing the experimental spectra to equal integrated intensity over the 4f multiplet, irrespective to the light polarization used. (For $L \neq 0$ one would need to rely on the often less precise normalization

procedures involving the PE background intensities or the photon flux).

In order to distinguish between surface and bulk contributions, which are not fully separated in energy, and to extract their relative intensities, the spectra have to be fitted. To perform a quantitative analysis, one has to keep in mind that the experiment is never performed under ideal conditions; the most important factors are: incomplete light polarization, finite temperature of the sample and the need to perform the PE measurements in remanence. As a consequence, the spectra will contain other contributions than theoretically expected for the 'ideal geometry'. These contributions are difficult to estimate, but they are expected to be equal in both spectra, i.e. they should cancel in the difference spectrum (see Fig. 5.2). This is an important advantage of using the 'difference' spectrum in the analysis (as compared to the 'parallel' and 'antiparallel' spectra for opposite magnetizations).

It is clear from the equal integrated intensities of the Gd-4f multiplets for $\Delta M = +1$ and $\Delta M = +1$ that the difference spectrum (MCD spectrum) vanishes when integrated over the whole multiplet. This property allows one to check the quality of the experimental data: the integrated area under the MCD spectrum should be equal to zero and the flanks should asymptotically approach zero.

The difference of the experimental spectra is plotted in the panel of Fig. 5.2. Owing to the surface core-level shift, the surface and bulk components are clearly visible also in the difference spectrum. This suggests that the shape of the spectrum corresponds to the sum of two MCD fundamental spectra shifted in binding energy. Owing to the proportionality between the I^1 fundamental spectrum intensity and the magnetization, we can expect that an extraction of layer-resolved information on the orientation of the 4f moments is possible.

For a quantitative spectral analysis we performed simultaneous least-squares fits of the dichroic difference spectrum and the sum of the spectra for opposite magnetizations. The results are shown in Fig. 5.3. Each of the Gd-4f 7F photoemission multiplets for the surface and sub-surface ('bulk') layers comprises seven spin-orbit components that cannot be resolved owing to the lifetime widths; yet the relative spectral intensities of the components are well known. The multiplet shape of the difference spectrum is described according to an expression derived from atomic multiplet theory. Accurate relative energy positions of lines within the multiplet were taken from optical data on Eu [62], and expanded to account for the larger spin-orbit parameter (due to the higher nuclear charge). The shapes of the individual multiplet components were described by the Doniach-Sunjic line shape.

The main contribution to each component is the fundamental spectrum I^1. Unlike magnetic dichroism in absorption (XMCD), the MD spectra in angle-resolved PE contain higher-order components that are not proportional to the magnetization (cf. Section 4.4). They have to be included in the fit analysis. The small correction in Fig. 5.3 accounts for contributions from the I^3-spectrum.

For normalization purposes the sum of the spectra was simultaneously fitted with the same parameters used for the difference spectrum. The shape of the multiplet was fitted with surface and bulk components for $\Delta M = \pm 1$ transitions

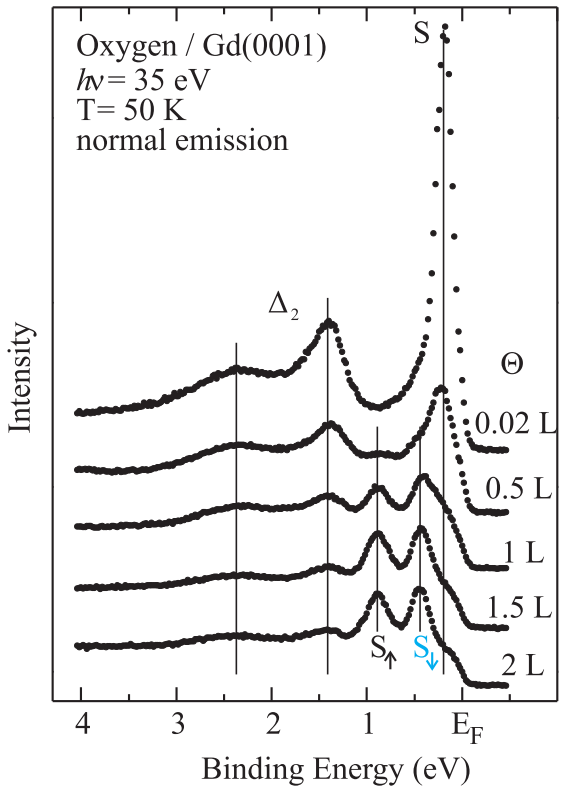

Figure 5.4: Development of the valence band due to oxygen adsorption on Gd(0001); the oxygen exposure is given in Langmuir (L). While the surface state of Gd is suppressed, two new oxygen-induced surface states appear at slightly higher binding energies; from Ref. [63].

(within a small $\Delta M = 0$ correction). The smoothly varying line describes the background of inelastically scattered electrons.

The intensity ratio of bulk and surface components in the difference spectrum is found to be 0.8. In the sum spectra, the surface-to-bulk intensity ratio is also 0.8. Hence, surface and bulk have the same magnetization projection onto the light axis (The estimated accuracy of this method is 10 %). Assuming ferromagnetic order for the bulk atoms, as widely accepted for 10-nm Gd films at 30 K, the present result strongly supports the view of a ferromagnetic alignment of the 4f moments in the outermost surface layer with respect to the underlying subsurface ('bulk') layers.

5.2 Oxygen adsorption on Gd(0001)

Studying the influence of adsorbates on single-crystal surfaces can provide valuable insights into the surface electronic structure, which may give a better understanding of surface magnetism of rare-earth metals. Such experiments were reported for hydrogen [64], oxygen [63, 65], and nitrogen [66] adsorption on

clean gadolinium surfaces. Clear suppression of the surface state is reported, but little information has been obtained about the magnetic properties. In a spin-polarized PE study of oxygen adsorption on Gd(0001), a suppression of surface magnetization was observed [67]. This finding was explained by the loss of delocalized conduction electrons upon oxidation and a concomitant reduction of magnetic coupling strength [67].

In this context, recently discovered well-ordered surface monoxides on heavy lanthanide metals [63, 68], in particular on Gd(0001) and Tb(0001), stimulate a study of their magnetic properties. Particularly interesting is the magnetic coupling of the surface-oxide layers with respect to the ferromagnetically ordered bulk. We note that antiferromagnetism also prevails in Gd-oxide bulk phases so that one may expect to encounter a competition between antiferro- and ferromagnetic exchange coupling for the present lanthanide surface monoxides. Such a competition had been reported for the epitaxial monolayer of Eu on Gd(0001), where it was suggested that a ferromagnetic Eu-Gd coupling leads to a non-vanishing Eu net magnetization [43, 69].

The effect of oxygen adsorption on the Gd(0001) surface is illustrated in Fig. 5.4. In our experiments oxygen was deposited at low temperatures; as well as at room temperature, but no difference was observed in the associated PE spectra. The subsequent annealing as well as the amount of oxygen exposure were found to be critical in preparing the $p(1 \times 1)O/Gd(0001)$ system. The annealing procedure requires great precision due to the low thermal stability of the adsorbate. We investigated two cases: (i) The system was prepared by exposure to 1 L oxygen with subsequent annealing at 300 K. (ii) It was prepared by exposure to 2L oxygen and subsequent annealing at 350 K; higher annealing temperatures imply the risk of oxygen desorption. In contrast, Tb surface monoxide reveals a higher stability, allowing higher annealing temperatures (up to 400 K), probably resulting in a better-ordered structure.

From previous studies it was concluded that oxygen adsorbs dissociatively with the creation of surface monoxide [63]. Moreover, from work-function measurements it was concluded that the oxygen adsorption site is below the Gd surface layer, i.e. "sub-surface" [65]. First principles band-structure calculations by Bihlmayer reveal a large outward relaxation of the surface layer (18 %), and they show no big difference in the binding energies for fcc and hcp adsorption sites of the oxygen atom [70]. Comparing our present experimental data for valence-band dispersion and 4f core-levels shift with the calculations, we clearly favor the on-top position of the oxygen atoms rather than the sub-surface position.

In agreement with previous studies by Meier and Schuessler-Langeheine [63, 71], we observed a suppression of the surface state of Gd, together with the formation of two new oxygen-induced states. We could reproduce the monotonic spectral variation with increasing oxygen dose, as shown in Fig. 5.4. However, the previous conclusion, that there is saturation of the surface after adsorption of 1 L of oxygen [63], can not be supported, as we find changes in the magnetic structure of the Gd 4f moments for doses above 1 L, as will be shown to from the MD studies described below.

The low stability of the monoxide indicates a weak binding between oxygen

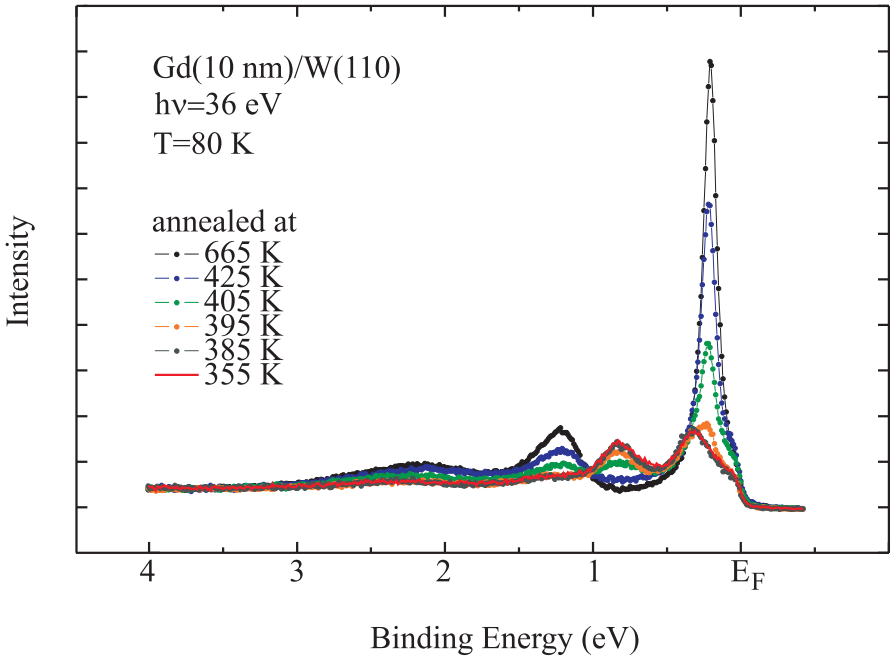

Figure 5.5: Modification of the valence band of 1-ML O/Gd(0001) upon annealing at different temperatures, illustrating the recovery of the metallic character of the surface.

and gadolinium atoms in this system. It implies the risk of degradation of the system by over annealing or by X-ray illumination. The temperature stability of the surface monoxide is displayed in Fig. 5.5, which shows a series of $p(1 \times 1)O/Gd(0001)$ spectra after annealing at different temperatures. Annealing at up to 385 K induces no spectral changes. But, starting from 395 K, there is a clear indication of oxygen desorption or its solution in the bulk. The surface state as well as the bulk bands are smoothly restored giving evidence of a practically clean Gd metal surface upon annealing at 665 K.

4f PE spectra recorded with CP polarized light of the system prepared with 1 L oxygen exposure at room temperature, are presented in Fig. 5.6. In the upper part, the spectra corresponding to $\Delta M = +1$ and $\Delta M = -1$ transitions are shown; the difference spectrum is plotted in the lower part. Upon formation of the surface monoxide, the surface core-level shift increases to 0.6 eV. This chemical shift allows one to separate the topmost surface layer from the atomic layers underneath, similar to the clean Gd(0001) surface. Without further analysis, the difference of the two spectra, the so-called 'dichroic' spectrum in Fig. 5.6, reveals a non-zero dichroic signal, at the position of the surface component. This shows that there is a non-vanishing net magnetization in the topmost atomic layer of O/Gd.

For a more quantitative spectral analysis we performed a least-squares fit analysis, with the results presented in Fig. 5.7. The surface component is considerably broader due to the intrinsic line width and maybe also due to

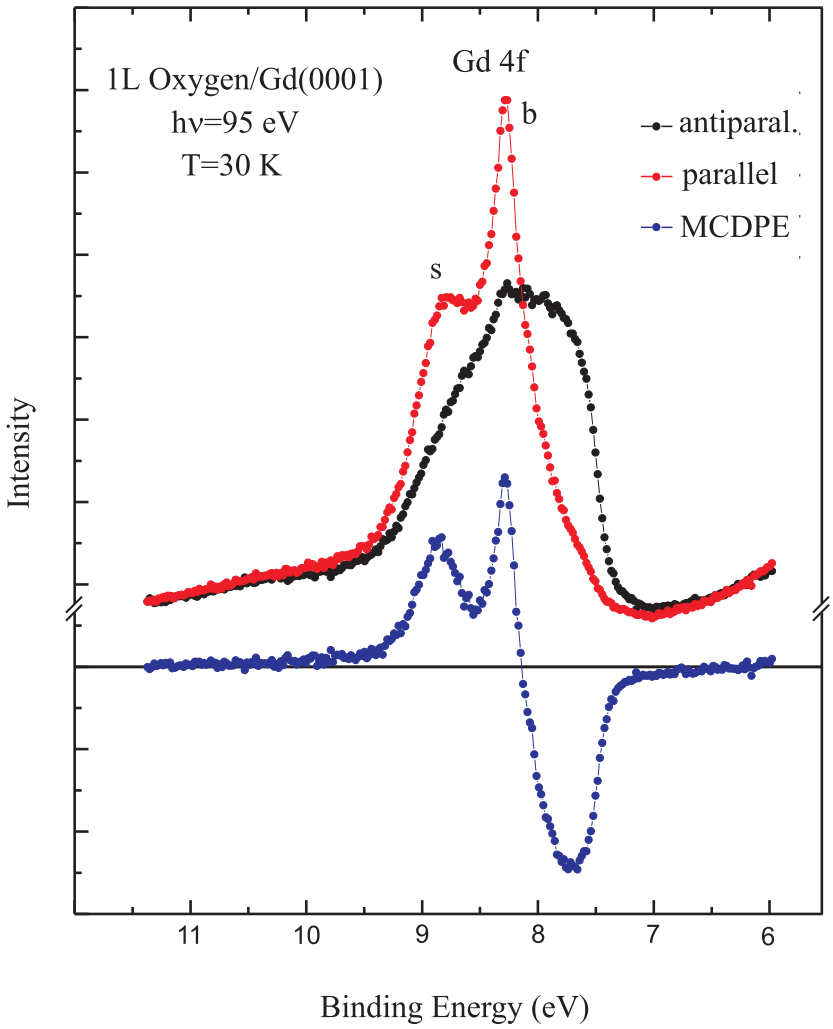

Figure 5.6: 4f-PE spectra of the O/Gd(0001) surface with surface (marked s) and bulk (marked b) components from an in-plane magnetized thin film recorded with circularly polarized light (light incidence angle $\theta^{h\nu} = 15°$, acceptance angle of electron analyzer $\alpha = \pm 14°$). Red (black) symbols represent parallel (antiparallel) orientation of sample magnetization and photon spin. The difference spectrum, calculated from the raw experimental data, is shown in the lower part of the figure.

imperfect structural order. The intensity ratio between the surface and bulk components in the difference spectrum is about 0.5. The sum spectra used for the normalization gives a surface-to-bulk intensity ratio of $\simeq$0.9. As a result, we arrive at a ratio of the normalized magnetization projections of the surface and bulk components of 0.56 (with 10 % accuracy). In other words, we observe a reduction of the surface magnetization by a factor of $\simeq$2 as compared to the clean Gd metal surface. Note, that the method is not sensitive to any hypothetical out-of-plane component of magnetization; however, a rotation of

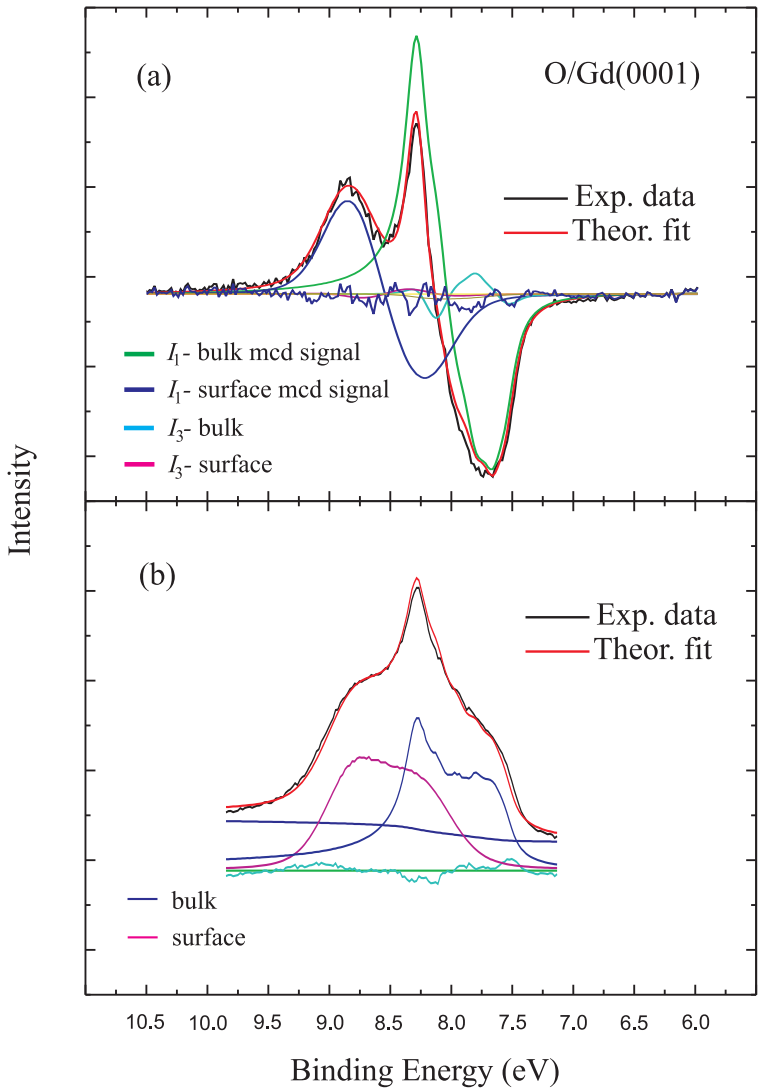

Figure 5.7: (a) Simultaneous least-squares fit analysis of the difference 4f-PE spectrum (from Fig. 5.6) of the O/Gd(0001) surface. Similar to Fig. 5.3, the experimental data is given by a solid black curve; fit result by a thin red curve; the residuum by a blue curve (the noisy curve represents approx. the zero line). (b) Fit analysis of the sum of the spectra in Fig. 5.6 similar to the case of clean Gd(0001) used for normalization of the components extracted from the dichroic spectra.

the surface magnetization with respect to the underlying "bulk" layers does not seem likely.

In the present $O/Gd(0001)$ system, the surface-layer magnetization was found to be dependent on annealing temperature and on the amount of the oxygen exposure. A second system was prepared by exposure to 2 L of oxygen followed by gentle annealing at 350 K to reach a saturation behavior of the

surface monoxide coverage.

Its magnetic structure was analyzed by means of MD in an analogous way as that of the first films, but with linearly-polarized light (LP) light in this case. MLD spectra of the 4f multiplets, recorded at off-normal emission direction, are shown on Fig. 5.8, with the difference spectrum plotted in the lower part. In contrast to MCD discussed above, the MLD effect at this photon energy arises solely from diffraction of the outgoing photoelectron ($g-$) waves, as will be shown in the next chapter. For a quantitative analysis, one has to take off-normal emission spectra. This is done in order to avoid a highly symmetrical geometry for the emission direction (cf. Chapter 6). In order to compare with previous results, the MLD spectra of the clean Gd(0001) metal surface were also taken and are presented in the inset.

The surface and bulk peaks in the 2-L PE spectra have not moved as compared to the previous system (1L of oxygen on Gd(0001)) and the surface core-level shift remains at 0.6 eV. It is striking, however, that there is practically no change in intensity of the surface component upon magnetization reversal, i.e. there is no dichroic signal in the surface component. In the difference spectrum, the bulk component reveals a dichroic signal of about 30 % with respect to the bulk peak intensity, and the dichroic signal of the surface component is clearly suppressed. This means that there is practically no ferromagnetic order in the outermost surface layer. This observation suggests an antiferromagnetic structure in the surface layer, with vanishing projection on the direction given by the photon wave vector.

Since oxygen is expected to strongly modify the electronic structure of the surface of the RE metals, we may raise the question regarding its possible influence on the subsurface layer. Proceeding in the same way as before, the amplitude of the difference spectrum for the bulk component normalized to intensity of the sum of the spectra can be defined. Its value is about 0.29. It can be compared with the amplitude of the MD signal from the bulk line of a clean Gd metal surface; this is shown in the inset of Fig. 5.8. For the normalized bulk MLD signal, the intensity ratio was found to be 0.26. If we assume that the bulk layers have a simple ferromagnetic structure, a comparison of the values indicates that a ferromagnetic structure in the second gadolinium layer of $p(1 \times 1)O/Gd(0001)$ is very likely to exist. The diffraction nature of the MLD signal reduces the accuracy of the quantitative analysis to 20 %.

The 20 % accuracy in this case is sufficient to distinguish between ferromagnetic and antiferromagnetic order. The simple formula $I = I_0 e^{-\frac{d}{\lambda}}$ describing the attenuation of the signal from the different layers shows that one will have a constant ratio between the signal from layer i and the sum of signals from deeper layers. Thus, from the 1:1 ratio of the intensities of the surface and bulk components (nonmagnetic sum of the spectra) follows that the same will hold for the ratio of the signals from the second layer and from all layers further inwards. For an antiferromagnetic ordering of the 4f moments in the second layer with respect to the bulk 4f moments, one would expect a reduction of the amplitude of the bulk MLD signal in $p(1 \times 1)O/Gd(0001)$ by a factor of two as compared to the amplitude of the bulk component in the MLD spectrum

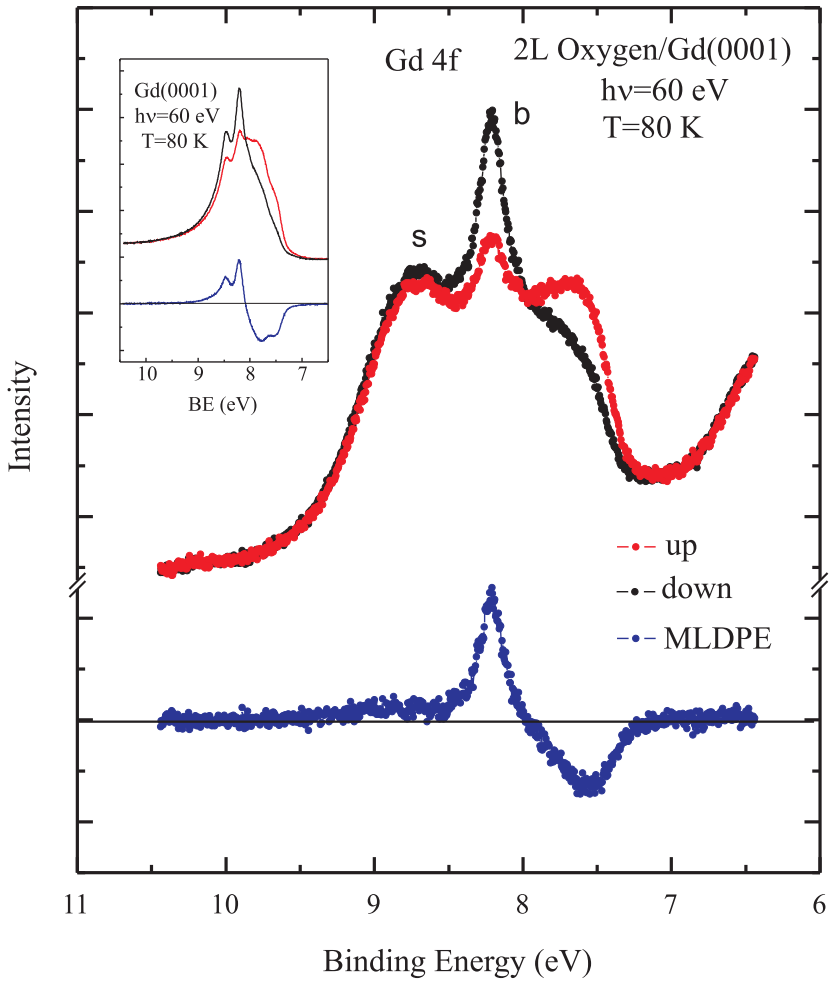

Figure 5.8: Off-normal PE spectra from $p(1\times1)O/Gd(0001)$, taken with linearly polarized light at 60-eV photon energy (off-normal angle of 2.46°, $\theta^{h\nu} = 35°$, acceptance angle of electron analyzer $\alpha = \pm 0.5°$), taken for two opposite magnetization directions perpendicular to the plane defined by the propagation direction of the incoming light and that of the outgoing photoelectrons. The difference spectrum is shown in the lower part; it is found to be very similar to dichroic spectra measured with circularly-polarized light in a planar experimental geometry. The inset shows MDPE spectra from a clean Gd(0001) surface taken at the same angle as the O/Gd(0001) spectrum for comparison.

of clean Gd. This is clearly not the case; the orientation of the 4f moments is rather parallel to the bulk moments. Also, an estimate from this formula results in a value of 4.5 Å for the electron mean-free path, i.e. a value that is quite reasonable for this photon energy.